Invertebrate Biology

Invertebrate Biology 137(3): 240–249.

DOI: 10.1111/ivb.12223

Vascular architecture in the bacteriogenic light organ of *Euprymna tasmanica* (Cephalopoda: Sepiolidae)

Anthony J. Patelunas and Michele K. Nishiguchi[a]

Department of Biology, New Mexico State University, Las Cruces, New Mexico 88003-8001, USA

Abstract. Symbiosis between southern dumpling squid, *Euprymna tasmanica* (Cephalopoda: Sepiolidae), and its luminescent symbiont, the bacterium *Vibrio fischeri*, provides an experimentally tractable system to examine interactions between the eukaryotic host and its bacterial partner. Luminescence emitted by the symbiotic bacteria provides light for the squid in a behavior termed "counter-illumination," which allows the squid to mask its shadow amidst downwelling moonlight. Although this association is beneficial, light generated from the bacteria requires large quantities of oxygen to maintain this energy-consuming reaction. Therefore, we examined the vascular network within the light organ of juveniles of *E. tasmanica* with and without *V. fischeri*. Vessel type, diameter, and location of vessels were measured. Although differences between symbiotic and aposymbiotic squid demonstrated that the presence of *V. fischeri* does not significantly influence the extent of vascular branching at early stages of symbiotic development, these finding do provide an atlas of blood vessel distribution in the organ. Thus, these results provide a framework to understand how beneficial bacteria influence the development of a eukaryotic closed vascular network and provide insight to the evolutionary developmental dynamics that form during mutualistic interactions.

Additional key words: symbiosis, squid, vasculature, aerobic

Symbiotic relationships between bacteria and multicellular organisms are very common in nature (Hirsch & McFall-Ngai 2000; Baker 2003; Wang et al. 2011). Beneficial symbioses occur when both members of the association benefit from their interactions with each other. These mutualistic relationships are observed in all major taxa including bacteria, plants, fungi, and metazoans (Leigh 2010; Wang et al. 2011; Zamborsky & Nishiguchi 2011). The relationships are highly integrated through the physiologies, metabolic capabilities, and genetic mechanisms that control either the symbiont, or are responsible for host changes to accommodate the symbiont (Bentley et al. 2013; Nadal & Paszkowski 2013; Tschaplinski et al. 2014). Additionally, presence of symbiotic organisms can influence developmental changes in the host, providing evidence of long-term coevolution between the partners (Bergsma & Martinez 2011; Dunlap et al. 2014; Koropatnick et al. 2014). For example, sepiolid squids (Cephalopoda: Sepiolidae) exemplify major morphogenic, biochemical, and physiological changes during infection and colonization by bacteria of the genus *Vibrio* from the environment (Montgomery & McFall-Ngai 1998; Foster et al. 2000; Koropatnick et al. 2014). Many of these changes are thought to prevent further colonization by additional environmental symbionts (Nyholm & McFall-Ngai 2004; Nyholm & Nishiguchi 2008; McFall-Ngai et al. 2010; Wier et al. 2010).

Changes in development can be observed and characterized by comparing symbiotic animals to aposymbiotic animals (Claes & Dunlap 2000; Foster et al. 2000; Koropatnick et al. 2004; Sycuro et al. 2006). Extensive vasculature in the light organ of the squid *Euprymna scolopes* was observed in earlier studies (McFall-Ngai & Montgomery 1990; Nyholm et al. 2009), but not mapped in detail. Although no hemocytes were tracked in this study, knowledge of how the vasculature develops may provide insight into where hemocytes enter the organ (as previously observed), or how they move to the crypts, invaginations of the light organ where the bacteria are housed, from the white body where they are produced (Nyholm et al. 2009; Kremer et al. 2014; Schwartzman et al. 2015).

[a]Author for correspondence.
E-mail: nish@nmsu.edu

The colonized light organ illuminates ventrally to match downwelling moonlight, camouflaging the squid from other benthic organisms during the night (Jones & Nishiguchi 2004). At dawn, the squid vents 90–95% of the bacteria from the organ into the surrounding seawater, with the remaining 5% re-colonizing the light organ throughout the day. This cycle is repeated daily for the life of the squid. Thus, squids benefit from the bioluminescence produced by the enzyme luciferase of their bacterial symbionts. The host squid in turn provide the bacteria with nutrients, and as a result they grow at least four times as fast in the squid light organ as they do in natural seawater (Lee & Ruby 1994), thereby increasing their overall fitness (Lee & Ruby 1994; Graf & Ruby 2000). While inside the crypts, colonies of *V. fischeri* produce light, which is regulated by expansion and contraction of the ink sac surrounding the light organ (Jones & Nishiguchi 2004). Production of luminescence via luciferase is aerobically intensive (Goto & Kishi 1968) and may capitalize on oxygen transferred through the squid's circulatory system. Thus, it is plausible that access to oxygen is a limitation to luminescence in the *Euprymna–Vibrio* symbiosis. Since very little is known about whether bacterial colonization induces change in the vasculature of sepiolid squids, the goal of this study was to compare the location and extent of vasculature between symbiotic and aposymbiotic light organs in *E. tasmanica*. Confocal scanning laser microscopy, as well as autofluorescence and Sca*l*e clearing agents (Hama et al. 2011), were used to examine the network of blood vessels in both aposymbiotic and symbiotic squids. The number of branching points (nodes) in each light organ was counted to analyze variation in branching. Diameters of vessels were measured and categorized to determine if there was a clear difference in vasodilation.

Methods

Adult animal collection and care

Adults of *Euprymna tasmanica* were collected from Botany Bay, New South Wales, Australia, with permits from the Australian Government, Department of Sustainability, Environment, Water, Population, and Communities (Export permit WT2013-10343), the New South Wales Government, Industry and Investment (Collection permit P04/0014-6.0), and the Australian Government Department of Agriculture, Fisheries, and Forestry Biosecurity (AQIS invoice ELS0016507329). *Euprymna tasmanica* was chosen as the model for this study due to the species' robustness and ease of rearing in captivity when compared to other species of sepiolids. Animals were transported back to NMSU, housed independently, and kept alive at the NMSU squid facility in a recirculating artificial seawater aquarium (100 L).

For mating, one male was added to a tank containing a female squid and an artificial cave (1/2 tube of 10 cm diameter PVC tube) in the evening. On the following mornings, caves were checked for deposition of eggs, and eggs (if present) were moved to a screened cage in a dedicated egg-rearing tank. Eggs were monitored daily for hatching, and animals were collected for experiments as soon as they hatched.

Experimental animal care

Laboratory-raised juveniles of *E. tasmanica* were maintained for up to 72 h (3 d) post-hatching in 5 mL of autoclave-sterilized artificial seawater (34 ppt; Instant Ocean©) in glass scintillation vials (one animal per vial; Nabhitabhata & Nishiguchi 2014). In a given clutch of eggs, newly hatched animals were assigned to symbiotic (to receive inoculated water) and aposymbiotic (no bacteria added) treatments. Symbiotic animals were infected by exposure to 5000 colony forming units (CFU) per mL of *V. fischeri* ETBB 10-1 for 12 h during the first water change on the first day post-hatching (Boettcher & Ruby 1995). Colonization of symbiotic animals was confirmed via presence of luminescence in a Berthold Sirius luminometer (Bethold Technologies, Bad Wildbad, Germany). Aposymbotic individuals were reared in seawater containing 5 $\mu g\ mL^{-1}$ chloramphenicol added once per week to prevent contamination. Animals were maintained with fresh sterilized seawater every 12 h. Squids were kept on a 12:12 h light: dark cycle.

Animals maintained for longer than 72 h were then transferred to 34 ppt autoclave-sterilized artificial seawater (Instant Ocean©) in 3-L glass bowls. Feeding did not occur before 72 h (3 d). One mysid shrimp per squid was placed in a 3-L glass bowl overnight for feeding. Prior to feeding, mysid shrimp were rinsed with autoclave-sterilized DI water, and then maintained in DI water until being placed in the bowl. Any remaining mysid shrimp were removed from the bowl the following morning.

All denoted experimental sampling time points are days post-hatching. Animals were sampled at 1, 4, and 14 d. The target collection was three individuals per time point for each experimental treatment.

Confocal microscopy

Juvenile squids were appropriately handled with care and under appropriate conditions to minimize any suffering (Nabhitabhata & Nishiguchi 2014). Juveniles were anesthetized on ice for 30 min in autoclave-sterilized artificial seawater, then fixed with 2.5% glutaraldehyde in 0.1 mol L^{-1} imidazole buffer for 48 h. After fixation, animal tissue was initially cleared with Sca*l*eA2 (4 mol L^{-1} urea, 10% glycerol, 0.1% Triton X-100) for 2 d, transferred to Sca*l*eB4 (8 mol L^{-1} urea, 10% glycerol, 0.1% Triton X-100) for an additional 2 d, and stored in Sca*l*eU2 (4 mol L^{-1} urea, 30% glycerol, 0.1% Triton X-100) at room temperature until imaging (Fig. 1A, B; (Hama et al. 2011). Clearing involves making tissue transparent and matching the refractive index throughout the tissue to the refractive index of the immersion media. Mantle cavities were opened from the ventral side, and the animal was decapitated directly behind the eyes with a stainless steel razor blade. Whole mantles were opened and placed ventral side down on a 35-mm MatTek glass-bottom dish (MatTek Corporation, Ashland, MA), embedded in 80% glycerol, and covered with a glass coverslip. Dissection, animal orientation, and stereoscopic imaging were completed on a Leica M165FC (Leica Microsystems, Wetzlar, Germany) stereofluorescent microscope.

Autofluorescence was imaged using a laser scanning confocal microscope (Leica TCS SP5 II, Leica Microsystems) with a 405-nm UV laser diode, a 488-nm argon-ion laser, and a 561-nm DPSS laser. Autofluorescent spectra for squid tissues were determined by generating λ scans for all available laser lines (Fig. 1C). A 40× 1.25 NA plan-apochromatic oil immersion lens was combined with linear compensation of the photomultiplier tubes and acousto-optic tunable filters, frame averaging, and stage-initiated tiling to generate a high-resolution mosaic of 3-μm optical sections. Blood vessels were identified by comparing region of interest (ROI) emission spectra with known vasculature in the gills (Fig. 2). Different from the surrounding tissue, the ROI spectra inside gill vessels match the ROI spectra inside blood vessels of the light organ. This information was used to infer which pieces of anatomy were blood vessels based on spectra and structural characteristics (tubular, branching, networking structures). Post-processing for confocal images was completed using ImageJ (National Institutes of Health, Bethesda, MD, USA) and Adobe Photoshop CS5 (Adobe Systems Inc., San Jose, CA, USA).

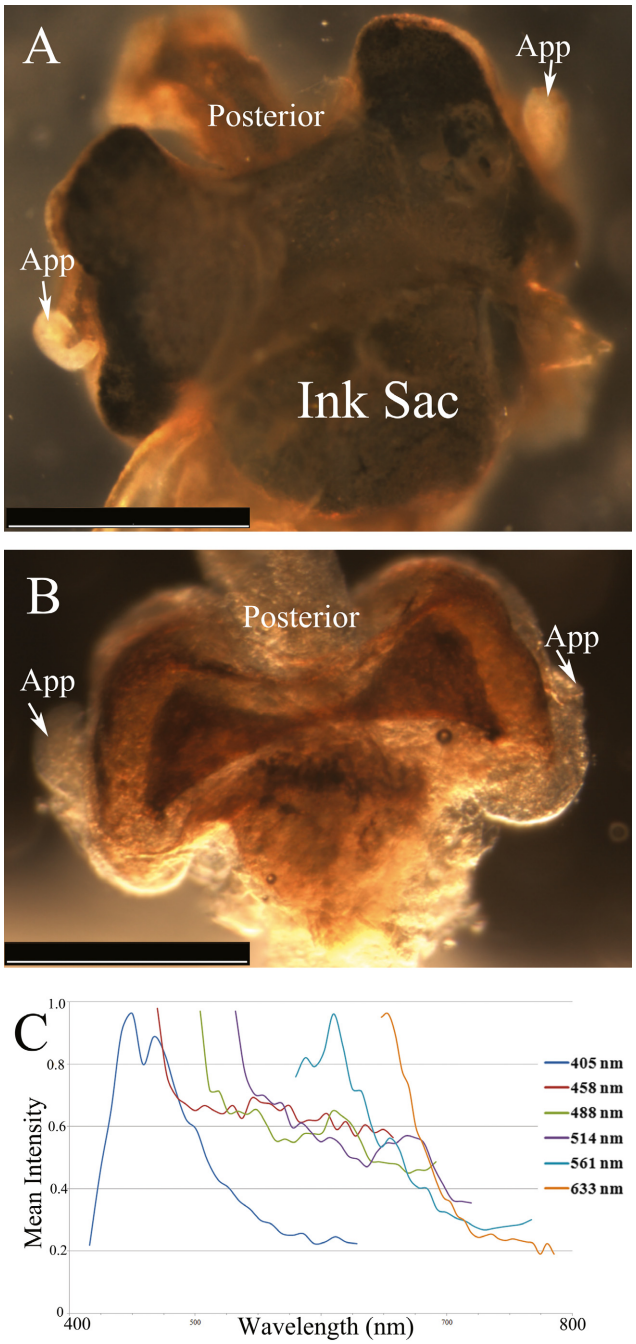

Fig. 1. Bright-field imaging and emission spectra from the light organ in 1 d juveniles of *Euprymna tasmanica*. **A**. Ventral view of an untreated juvenile light organ removed from the squid mantle cavity. Posterior portion of the animal is toward the top of the figure. **B.** Ventral view of a Sca*l*e-cleared light organ removed from the squid mantle cavity. Anterior portion of the animal is toward the top of the figure. **C.** Emission spectra controls for squid muscle tissue exhibiting normalized mean intensity (*y*-axis) over wavelength in nm (*x*-axis). The laser line used for the spectrum is in the top right corner of each graph. App, appendage. Scale bar=500 μm.

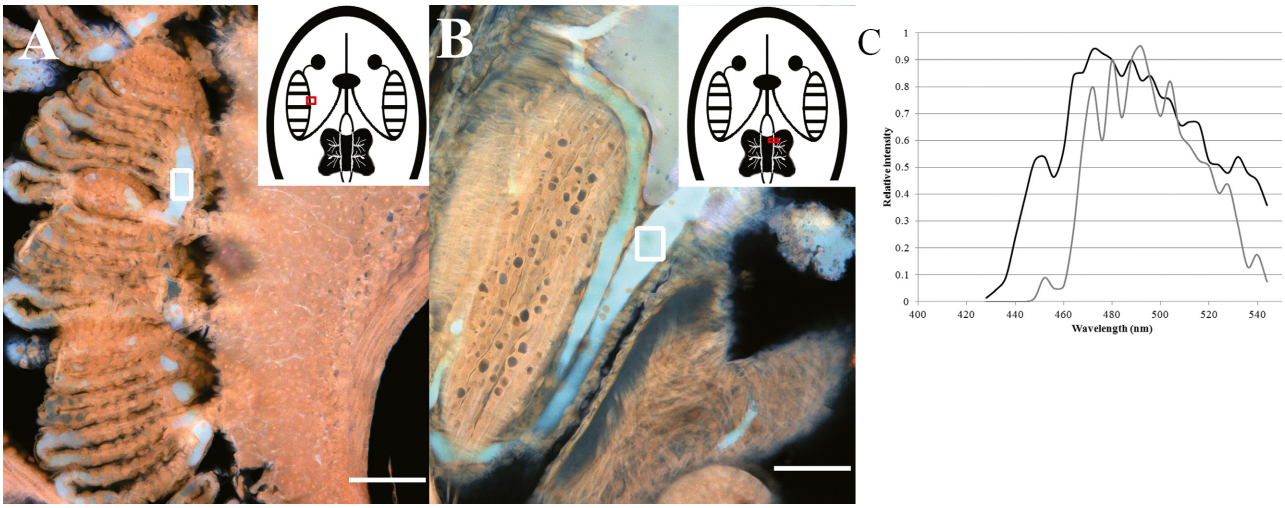

Fig. 2. Region of interest (ROI) λ scans of blood vessels in the gills (**A**) and in the light organ (**B**) of a 14 d juvenile of *Euprymna tasmanica*. **A**. Squid gill, XY optical section imaged with a 405-nm UV laser diode. The white box indicates the ROI scanned for the emission spectrum. **B**. Squid light organ, XY optical section of the central tissue in the light organ imaged with the 405-nm laser. The white box represents the ROI in which the emission spectrum was measured. **C.** Emission spectra for scans in (A) (black line) and (B) (gray line). Scale bar=100 μm.

Morphometric analysis

Diameters of blood vessels were measured manually before and after branch points with the straight-line tool in ImageJ, and means and standard error were calculated from measurements (Cartana et al. 2012). Measurements were taken from XY optical sections, and XZ and YZ orthogonal projections. Vessel branches were marked and counted to determine the number of nodes. A minimum of three animals were used for each treatment (symbiotic or aposymbiotic) for biological replicates at each time point (1, 4, 14 d). All vessels that could be traced were visualized for each animal. Animals were collected and fixed at noon for each of the respective time points. A one-way analysis of variance (ANOVA) was used to compare treatments at the same time point, and the same treatment between time points. P-values were corrected with the Holm–Bonferroni test (Holm 1979).

Results

Confocal microscopy

Vessels were divided into four categories based on position relative to the light organ and size: L, the large vessel that runs posterior to anterior; MA, the anterior branch from L going into either of the lobes of the bilobed light organ; MP, the posterior branch from L going into either of the lobes of the bilobed light organ; and S, the branches from MA or MP. Figures 3 and 4 show the position of each of these vessels. The L vessel was consistently on the ventral surface of the light organ, running proximally posterior to anterior, directly under the hindgut on either side. The MA and MP vessels formed a V-shaped structure, branching anterior and posterior, respectively. The S vessels were long and branched in no particular pattern. These vessels wrapped around the deep crypts (Fig. 4B,D,F,H,J,L).

Measurements

There were few significant differences between aposymbiotic and symbiotic squids in ANOVA comparisons over three time points; however, this analysis provided a descriptive map to the vascular network. The largest trends observed were increases in vessel size at the earliest (1 d) and latest (14 d) time points. Increases in node number happened between each time point, as expected during the early stages of development.

There were no differences between aposymbiotic and symbiotic squids in L, MA, or MP values from the right lobe of the light organ at the 1 d time point (Fig. 5, Table 1). Similarly, no differences were found between the two treatments in L, MA, and MP values at the 4 d time point. However, in 1 d samples, there was a significant difference between symbiotic and aposymbiotic animals in S

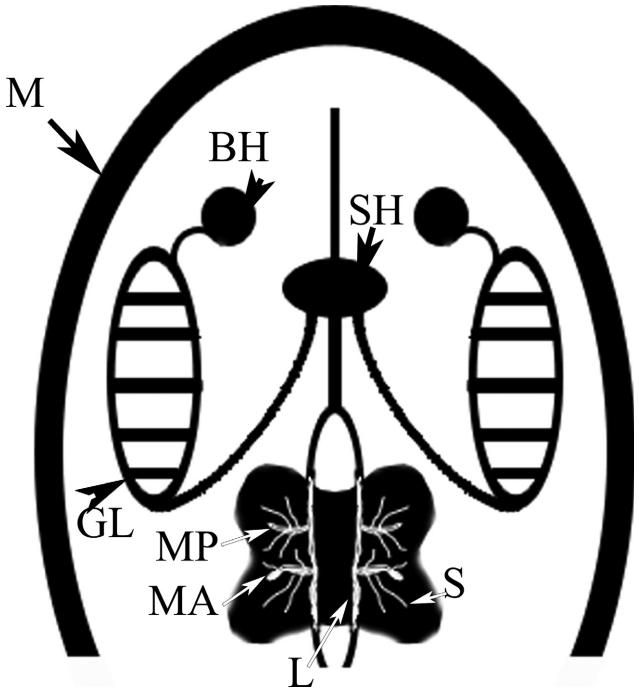

Fig. 3. A diagram proposing the orientation and hierarchy of blood vessels throughout the light organ, as described in this article. Posterior is to the top. GL, gill; L, the largest vessel that bifurcates to each lobe of the light organ; LO, light organ; M, mantle; MA, the anterior branch of the second tier of vessels; MP, the posterior branch of the second tier of vessels; S, the third tier of vessels that sprawls throughout the organ; SH, systemic heart.

measurements from the left lobe. Conversely, a difference in the number of nodes was observed in the 4 d samples, but not in the 1 d specimens. No major differences in measurements were observed between the two treatments in S vessels at the 14 d time point, but all other vessels (L, MA, MP) exhibited an increased size in symbiotic animals at the 14 d time point.

The MA and MP vessels from the left lobes of aposymbiotic and symbiotic squids at the 1 d time point were not significantly different (Table S1), but the L vessels from the left lobes were significantly larger in symbiotic animals after 1 d of development with symbionts. There were no significant differences between S vessels of the left and right lobes after 1 d. The number of nodes in the left lobe of 1 d samples was not similar.

There were no differences between treatments in any of the measurements from the left lobe after 4 d. However, comparison of time points within treatments had different results. When the 1 d aposymbiotic animal lobes were compared with the 4 d aposymbiotic animal lobes, MA diameter was not significantly different ($p=0.13$, right lobe; $p=0.95$, left lobe) but the number of nodes were significantly greater in the right lobe. We found large changes from 1 to 4 d in the size of S vessels of symbiotic animals ($p=0.0003$, right lobe; $p=0.003$, left lobe), which demonstrates fast growth.

When comparing the 14 d specimens, a significant increase in size was observed in the symbiotic L vessels when compared with the aposymbiotic treatment. Most interesting were the changes from the 4 d samples to the 14 d samples within treatment. Aposymbiotic squid exhibited no significant changes in the number of nodes ($p=0.09$ for R and $p=0.04$ for L), but symbiotic animals significantly increased the number of nodes ($p<0.00001$, right lobe; $p=0.003$, left lobe). No other significant differences were consistent between lobes.

Discussion

Oxygen delivery by individuals of *Euprymna tasmanica* to symbiotic colonies of *Vibrio fischeri* inhabiting the light organ is crucial for understanding the biochemical reactions that produce luminescence, which is necessary for a successful mutualism. Therefore, this study examined the extent of vascularization in the developing bacteriogenic light organ of *E. tasmanica* during early post-hatching development. Previous studies have demonstrated the presence of the blood vessels in adult squids (McFall-Ngai & Montgomery 1990; Nyholm et al. 2009), as well as anaerobic conditions inside the light organ (Ruby & McFall-Ngai 1999; Wier et al. 2010; Schwartzman et al. 2015). These studies provide evidence that the presence of *V. fischeri* in the light organ does not influence angiogenesis. Oxygen is required for the catalysis of luciferase during bioluminescence in *V. fischeri* (Goto 1968), and therefore needs to be present in large quantities to sustain bioluminescence, in addition to aerobic metabolism in both the symbionts and their host squid.

Although the number of branching events does not appear to be significantly different between aposymbiotic and symbiotic animals, there is a significant difference between treatments in the diameter of the S vessel in the left lobe in the 1 d samples (Fig. 5; Table 1). Within the first 24 h after inoculation with symbiotic bacteria, cell death occurs in the appendages and surface epithelial cells of the light organ (Foster et al. 2000; Koropatnick et al. 2014). Cells directly in contact with colonies of *V. fischeri* further differentiate, becoming cuboidal and increasing in size (Montgomery & McFall-Ngai 1994;

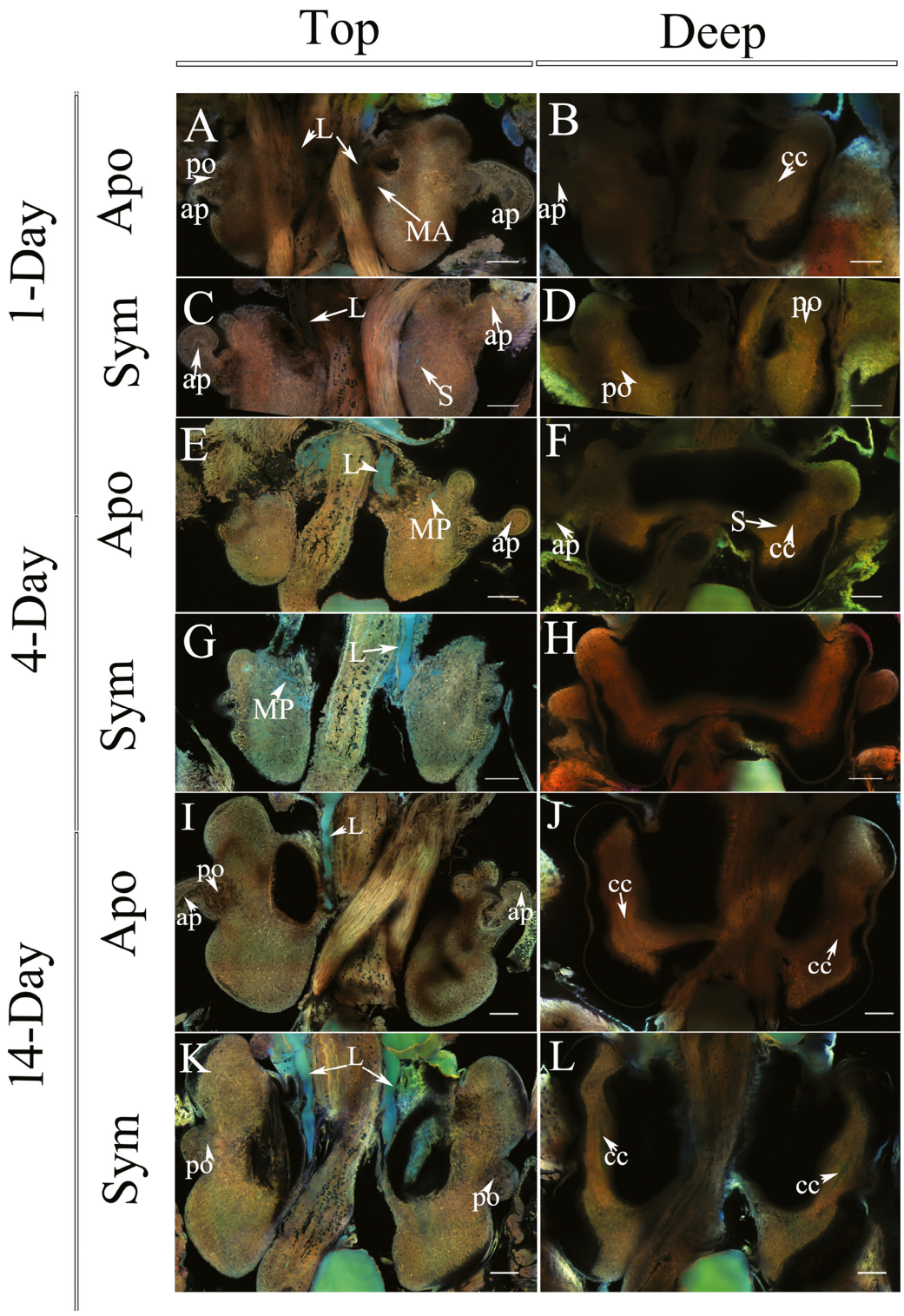

Fig. 4. Optical sections of each light organ treatment observed**.** Light organs are oriented from a ventral view with posterior at the top. All images are a merger of laser lines 405 nm (blue), 488 nm (green), and 561 nm (red). The column labeled "Top" represents shallow optical sections of the surface of the light organ and large vessel; the "Deep" column represents the deep crypts and associated vessels. **A–D**. 1 d aposymbiotic (A, B) and symbiotic (C, D) samples exhibiting light organ surface and deep crypts. **E–H**. 4 d aposymbiotic (A, B) and symbiotic (C, D) samples exhibiting light organ surface and deep crypts. **I–L.** 14 d aposymbiotic (A, B) and symbiotic (C, D) samples exhibiting light organ surface and deep crypts. ap, anterior appendage; cc, crypt; po, pore. Scale bars=100 μm.

Lamarcq & McFall-Ngai 1998; Sycuro et al. 2006). Since this is a vital time point for symbiont initiation, vasodilation might be initiated by the presence of colonies of *V. fischeri*. Nitric oxide (NO), which is known to be a vasodilator, is released during the early stages of the symbiosis as a defense against non-symbiotic bacteria accumulation. However, NO steadily decreases after the initial inoculation of bacteria (Davidson et al. 2004). In this study, there was no significant difference between treatments in any of the vessel diameters at the 4 d time point. Blood vessels will return to a resting diameter with a reduction in NO instead of being dilated, as observed in 1 d samples from the treatment with symbionts. This suggests that after symbiont establishment, delivery of substances in the hemolymph (nutrients, oxygen, hemocytes, etc.) is reduced to a pre-symbiotic state, similar to that of aposymbiotic animals. Alternatively, this difference could simply be an artifact of small sample size (n=3 for each set). Observations of how these vessels change with the development of larger colonies of *V. fischeri* during the height of their infection (at night), and around the time of venting (at dawn), might give additional insight into how specific vasodilators control blood vessel size during different stages of the mutualism.

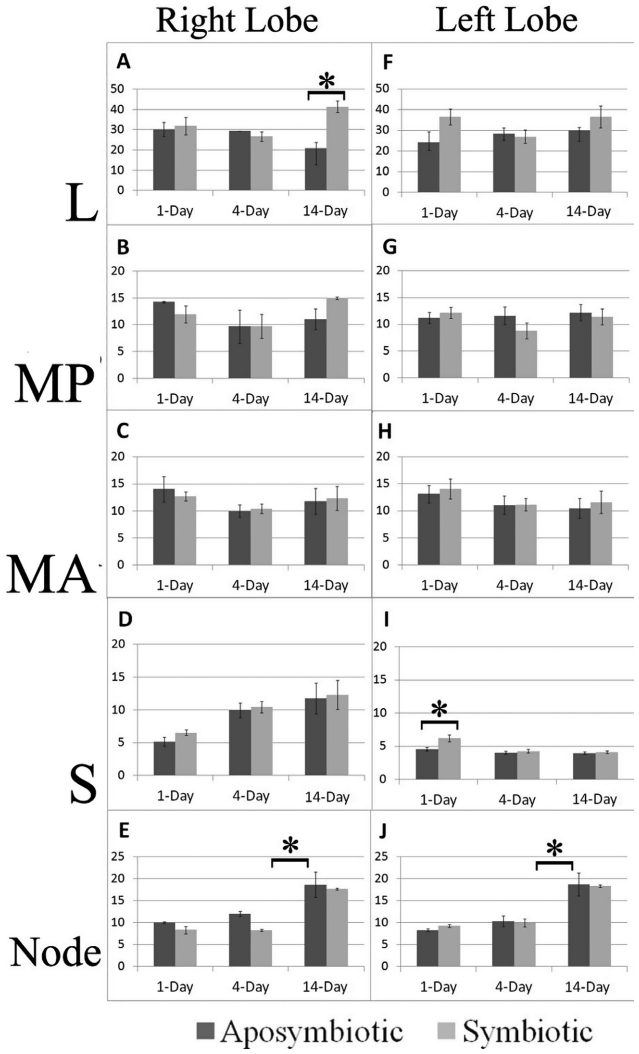

Fig. 5. Diameter of vessels (μm) in left and right lobes of the light organ of aposymbiotic and symbiotic animals. Animals from each treatment were sampled after 1, 4, or 14 d. Values are means ± standard error. **A,F.** L vessel. **B,G.** MP vessel. **C,H.** MA vessel. **D,I.** S vessel. **E,J.** Number of branch points (nodes) counted for each of the samples. Asterisk indicates significance at $p < 0.05$.

The lack of any difference in the number of nodes in the 1 d samples might be a result of developmental time. Angiogenesis induced by low oxygen levels requires continual anaerobic stress (Shweiki et al. 1992). If anaerobic stress is induced by the presence of colonies of *V. fischeri*, it would be during the period of highest oxygen demand, or during luminescence. This period only lasts a maximum of ~12 h during the night when symbionts are at their highest abundance in the light organ. In the squids exposed to symbionts for 1 d, a single ~12-h period may have been too short to generate differences in angiogenesis. Longer time points were examined to determine if developmental timing was influential on vascular growth (Fig. 4E–L). A significant difference between treatments was found in the number of nodes in right lobes after exposure for 4 d, but not in left lobes. This difference between lobes may be due to the small number of samples examined for each time point (n=3). However, this is not the only measurement that exhibited such a difference between lobes.

Differences between the right and left lobe can potentially be explained by asymmetric development in protostomes. Although it has not been extensively explored, left–right asymmetry during development has been observed in nematodes and pulmonate snails (Okumura et al. 2008). Mollusca as a group have evolved and lost symmetry numerous times throughout evolutionary history. Among cephalopods, the conversion from symmetry to asymmetry is estimated to have changed at least five times, with right and left bias evolving simultaneously (Palmer 1996). Light organs in the related congener *Semirossia* also share asymmetry in the ducts leading to the light organ (Boletzky 1970). This similarity may provide indirect evidence for the onset of morphological changes that induced development of the original light organ present in basal sepiolid squids

Table 1. Measurements of each lobe in aposymbiotic (apo) and symbiotic (sym) juvenile squids sampled after 1, 4, and 14 d.

	1 d apo	1 d sym	4 d apo	4 d sym	14 d apo	14 d sym
N	3	3	3	4	3	3
Right lobe						
Diameters of blood vessels (μm)						
L	30.02±3.42	31.83±4.32	29.46±0.21	26.71±2.32	20.92±8.08	41.40±2.89
MA	14.23±0.11	11.97±1.60	9.69±3.12	9.71±2.21	11.06±1.91	14.98±0.24
MP	14.05±2.35	12.71±0.87	9.95±1.15	10.45±0.84	11.78±2.39	12.33±2.22
S	5.17±0.66	6.56±0.40	4.75±0.25	4.23±0.23	4.15±0.15	4.40±0.16
Number of nodes	10.00±0.18	8.33±0.88	12.00±0.58	8.25±0.25	18.67±2.91	17.67±0.21
Left lobe						
Diameters of blood vessels (μm)						
L	24.28±5.14	36.56±3.85	28.38±2.95	26.93±3.24	30.12±1.31	36.57±5.36
MA	11.23±1.05	12.15±1.04	11.62±1.65	8.82±1.51	12.19±1.56	11.37±1.49
MP	13.12±1.60	14.05±1.82	11.06±1.74	11.15±1.16	10.46±1.82	11.61±2.07
S	4.59±0.26	6.22±0.51	4.02±0.23	4.29±0.25	3.97±0.18	4.13±0.17
Number of nodes	8.33±0.23	9.33±0.33	10.33±1.20	10.00±0.91	18.67±2.60	18.33±0.31

N, number of samples; L, large vessels; MA, medium anterior vessels; MP, medium posterior vessels; S, small vessels.

(such as *Semirossia*), and suggests a possible developmental origin for an organ in which bacteria, such as *V. fischeri*, could initiate a beneficial association (Naef, 1921; Nishiguchi et al. 2004).

Imaging of juvenile squids shows that the posterior aorta branches to feed blood into the light organ. This pathway has been previously observed in *Semirossia tenera* (Boletzky 1970). Afferent vessels enter the light organ on the ventral side (Figs. 3, 4A–L) to either side of the hindgut. Our study confirms the vascular anatomical similarities in light organs between distantly related symbiotic squid (Nishiguchi et al. 2004). Host squids may increase oxygen delivery, and thereby compensate for a decreased node number or lack of change in vessel diameter, by elevating their heart rate. Future projects might investigate the rate or volume output of the systemic heart, since increase output may be an alternative way to deliver an increased supply of oxygen and nutrients to the light organ (Intaglietta et al. 1996). Additionally, vessel diameter can be examined at varying *in vivo* time points to determine whether the changes in diameter are associated with daily variation in metabolic activity of the squids.

By examining morphological changes between aposymbiotic and symbiotic sepiolid squids, this study has provided further insights into the mechanisms behind beneficial mutualisms. Additionally, by understanding the location and extent of vascular anatomy in the light organ, the role of hemocyte migration into the crypts can be tracked and analyzed. Other symbiotic systems have demonstrated nutrient exchange between symbiotic partners (Baker 2003; Denison & Kiers 2011), and only recently has oxygen transfer in the sepiolid squid begun to be explored (Kremer et al. 2014). These results demonstrate that the circulatory system in *E. tasmanica* develops similarly in both symbiotic and aposymbiotic juveniles, regardless of the presence of colonies of *V. fischeri*; however, the functional changes associated with the presence of *V. fischeri* remain to be determined. Live confirmation of vasodilation in the early stages of the symbiosis would provide additional information regarding the development of this association. A thorough understanding of how the vascular system adapts under the stress of maintaining a symbiosis provides a starting point for testing the innate immune response on an organismal scale, and an alternative hypothesis for the role of a circulatory system in maintaining beneficial associations such as vertebrate gut microbes.

Acknowledgments. The authors thank P. H. Cook at the NMSU CURRL facility for help with all microscopy. This work was supported by NIH NIAID 1SC1AI081659, NIH NIAIDS 3SC1AI081659-02S1, and NSF IOS 074498 to M.K.N. This study was carried out in strict accordance with the recommendations in the Guide for the Care and Use of Laboratory Animals of the National Institutes of Health. The protocol was approved by the Institutional Biosafety Committee of New Mexico State University (permit number: 1306NMD20103) and under the guidelines of the NMSU's Institutional Animal Care and Use

Committee (85-R-009 and OLAW A4022-01 and IACUC license 2013-029).

References

Baker AC 2003. Flexibility and specificity in coral-algal symbiosis: Diversity, ecology, and biogeography of *Symbiodinium*. Annu. Rev. Ecol. Evol. Syst. 34: 661–689.

Bentley K, Jones M, & Cruys B 2013. Predicting the future: towards symbiotic computational and experimental angiogenesis research. Exp. Cell Res. 319: 1240–1246.

Bergsma GS & Martinez CM 2011. Mutualist-induced morphological changes enhance growth and survival of corals. Mar. Biol. 158: 2267–2277.

Boettcher KJ & Ruby EG 1995. Detection and quantification of *Vibrio fischeri* autoinducer from symbiotic squid light organs. J. Bacteriol. 177: 1053–1058.

Boletzky SV 1970. On presence of light organs in *Semirossia* Steenstrup, 1887 (Mollusca - Cephalopoda). Bull. Mar. Sci. 20: 374.

Cartana T, Saftoiu A, Gruionu LG, Gheonea DI, Pirici D, Georgescu CV, Ciocalteu A, & Gruionu G. 2012. Confocal laser endomicroscopy for the morphometric evaluation of microvessels in human colorectal cancer using targeted anti-CS1 antibodies. PLoS ONE 7(12): e52815. http://doi.org/10.1371/journal.pone.0052815.

Claes MF & Dunlap PV 2000. Aposymbiotic culture of the sepiolid squid *Euprymna scolopes:* role of the symbiotic bacterium *Vibrio fischeri* in host animal growth, development, and light organ morphogenesis. J. Exp. Zool. 286: 280–296.

Davidson SK, Koropatnick TA, Kossmehl R, Sycuro L, & McFall-Ngai MJ 2004. NO means 'yes' in the squid-vibrio symbiosis: nitric oxide (NO) during the initial stages of a beneficial association. Cell. Microbiol. 6: 1139–1151.

Denison RF & Kiers ET 2011. Life histories of symbiotic rhizobia and mycorrhizal fungi. Curr. Biol. 21: R775–R785.

Dunlap PV, Takami M, Wakatsuki S, Hendry TA, Sezaki K, & Fukui A 2014. Inception of bioluminescent symbiosis in early developmental stages of the deep-sea fish, *Coelorinchus kishinouyei* (Gadiformes: Macrouridae). Ichthyol. Res. 61: 59–67.

Foster JS, Apicella MA, & McFall-Ngai MJ 2000. *Vibrio fischeri* lipopolysaccharide induces developmental apoptosis, but not complete morphogenesis, of the *Euprymna scolopes* symbiotic light organ. Dev. Biol. 226: 242–254.

Goto T 1968. Chemistry of bioluminescence. Pure Appl. Chem. 17: 421–442.

Goto T & Kishi Y 1968. Luciferins bioluminescent substances. Angew. Chem.-Int. Edit. 7: 407.

Graf J & Ruby EG 2000. Novel effects of a transposon insertion in the *Vibrio fischeri glnD* gene: defects in iron uptake and symbiotic persistence in addition to nitrogen utilization. Mol. Microbiol. 37: 168–179.

Hama H, Kurokawa H, Kawano H, Ando R, Shimogori T, Noda H, Fukami K, Sakaue-Sawano A, & Miyawaki A 2011. Scale: a chemical approach for fluorescence imaging and reconstruction of transparent mouse brain. Nat. Neurosci. 14: 1481-U166.

Hirsch AM & McFall-Ngai MJ 2000. Fundamental concepts in symbiotic interactions: light and dark, day and night, squid and legume. J. Plant Growth Regul. 19: 113–130.

Holm S 1979. A simple sequentially rejective multiple test procedure. Scand. J. Stat. 6: 65–70.

Intaglietta M, Johnson PC, & Winslow RM 1996. Microvascular and tissue oxygen distribution. Cardiovasc. Res. 32: 632–643.

Jones BW & Nishiguchi MK 2004. Counterillumination in the Hawaiian bobtail squid, *Euprymna scolopes*; Berry (Mollusca: Cephalopoda). Mar. Biol. 144: 1151–1155.

Koropatnick TA, Engle JT, Apicella MA, Stabb EV, Goldman WE, & McFall-Ngai MJ 2004. Microbial factor-mediated development in a host-bacterial mutualism. Science 306: 1186–1188.

Koropatnick T, Goodson MS, Heath-Heckman EA, & McFall-Ngai M 2014. Identifying the cellular mechanisms of symbiont-induced epithelial morphogenesis in the squid-*Vibrio* association. Biol. Bull. 226: 56–68.

Kremer N, Schwartzman J, Augustin R, Zhou L, Ruby EG, Hourdez S, & McFall-Ngai MJ 2014. The dual nature of haemocyanin in the establishment and persistence of the squid-*Vibrio* symbiosis. Proc. Biol. Sci. Roy. Soc. 281: 20140504.

Lamarcq LH & McFall-Ngai MJ 1998. Induction of a gradual, reversible morphogenesis of its host's epithelial brush border by *Vibrio fischeri*. Infect. Immun. 66: 777–785.

Lee KH & Ruby EG 1994. Effect of the squid host on the abundance and distribution of symbiotic *Vibrio fischeri* in nature. Appl. Environ. Microbiol. 60: 1565–1571.

Leigh EG 2010. The evolution of mutualism. J. Evol. Biol. 23: 2507–2528.

McFall-Ngai M & Montgomery MK 1990. The anatomy and morphology of the adult bacterial light organ of *Euprymna scolopes* Berry (Cephalopoda, Sepiolidae). Biol. Bull. 179: 332–339.

McFall-Ngai M, Nyholm SV, & Castillo MG 2010. The role of the immune system in the initiation and persistence of the *Euprymna scolopes-Vibrio fischeri* symbiosis. Sem. Immunol. 22: 48–53.

Montgomery MK & McFall-Ngai M 1994. Bacterial symbionts induce host organ morphogenesis during early postembryonic development of the squid *Eurpymna scolopes*. Development 120: 1719–1729.

Montgomery MK & McFall-Ngai MJ 1998. Late postembryonic development of the symbiotic light organ of *Euprymna scolopes* (Cephalopoda: Sepiolidae). Biol. Bull. 195: 326–336.

Nabhitabhata J & Nishiguchi MK 2014. *Euprymna hyllebergi* and *Euprymna tasmanica*. In: Cephalopod

Culture, Iglesias J, Fuentes L & Villanueva R, eds., pp. 253–269. Springer, The Netherlands.
Nadal M & Paszkowski U 2013. Polyphony in the rhizosphere: presymbiotic communication in arbuscular mycorrhizal symbiosis. Curr. Opin. Plant Biol. 16: 473–479.
Naef A 1921. Die Cephalopoden, I. Teil. Berlin: R. Friedländer & Sohn, 1921–1928.
Nishiguchi MK, Lopez JE, & von Boletzky S 2004. Enlightenment of old ideas from new investigations: more questions regarding the evolution of bacteriogenic light organs in squids. Evol. Dev. 6: 41–49.
Nyholm SV & McFall-Ngai MJ 2004. The winnowing: establishing the squid-*Vibrio* symbiosis. Nat. Rev. Microbiol. 2: 632–642.
Nyholm SV & Nishiguchi MK 2008. The evolutionary ecology of a Sepiolid squid-*Vibrio* association: from cell to environment. Vie Et Milieu-Life Environ. 58: 175–184.
Nyholm SV, Stewart JJ, Ruby EG, & McFall-Ngai MJ 2009. Recognition between symbiotic *Vibrio fischeri* and the haemocytes of *Euprymna scolopes*. Environ. Microbiol. 11: 483–493.
Okumura T, Utsuno H, Kuroda J, Gittenberger E, Asami T, & Matsuno K 2008. The development and evolution of left-right asymmetry in invertebrates: lessons from *Drosophila* and snails. Dev. Dyn. 237: 3497–3515.
Palmer AR 1996. From symmetry to asymmetry: phylogenetic patterns of asymmetry variation in animals and their evolutionary significance. Proc. Natl Acad. Sci. USA 93: 14279–14286.
Ruby EG & McFall-Ngai MJ 1999. Oxygen-utilizing reactions and symbiotic colonization of the squid light organ by *Vibrio fischeri*. Trends Microbiol. 7: 414–420.
Schwartzman JA, Koch E, Heath-Heckman EAC, Zhou L, Kremer N, McFall-Ngai MJ, & Ruby EG 2015. The chemistry of negotiation: rhythmic, glycan-driven acidification in a symbiotic conversation. Proc. Natl Acad. Sci. USA 112: 566–571.
Shweiki D, Itin A, Soffer D, & Keshet E 1992. Vascular endothelial growth-factor induced by hypoxia may mediate hypoxia-initiated angiogenesis. Nature 359: 843–845.
Sycuro LK, Ruby EG, & McFall-Ngai M 2006. Confocal microscopy of the light organ crypts in juvenile *Euprymna scolopes* reveals their morphological complexity and dynamic function in symbiosis. J. Morphol. 267: 555–568.
Tschaplinski TJ, Plett JM, Engle NL, Deveau A, Cushman KC, Martin MZ, Doktycz MJ, Tuskan GA, Brun A, Kohler A, & Martin F 2014. *Populus trichocarpa* and *Populus deltoides* exhibit different metabolomic responses to colonization by the symbiotic fungus *Laccaria bicolor*. Mol. Plant-Microbe Interact. 27: 546–556.
Wang XR, Pan QA, Chen FX, Yan XL, & Liao H 2011. Effects of co-inoculation with arbuscular mycorrhizal fungi and rhizobia on soybean growth as related to root architecture and availability of N and P. Mycorrhiza 21: 173–181.
Wier AM, Nyholm SV, Mandel MJ, Massengo-Tiasse RP, Schaefer AL, Koroleva I, Splinter-BonDurant S, Brown B, Manzella L, Snir E, Almabrazi H, Scheetz TE, Bonaldo MD, Casavant TL, Soares MB, Cronan JE, Reed JL, Ruby EG, & McFall-Ngai MJ 2010. Transcriptional patterns in both host and bacterium underlie a daily rhythm of anatomical and metabolic change in a beneficial symbiosis. Proc. Natl Acad. Sci. USA 107: 2259–2264.
Zamborsky DJ & Nishiguchi MK 2011. Phylogeographical patterns among Mediterranean sepiolid squids and their *Vibrio* symbionts: environment drives specificity among sympatric species. Appl. Environ. Microbiol. 77: 642–649.

Supporting information

Additional supporting information may be found online in the Supporting Information section at the end of the article:

Table S1. Statistical comparisons of vessel sizes from squid exposed to symbiotic and aposymbiotic treatments.